Dynamical Calculation of the $\frac{3}{2}^+$ Resonance Spectrum and $SU(3)$ Symmetry Breaking*

J. KATZ† AND S. WAGNER
II. Institut für Theoretische Physik der Universität Hamburg, Hamburg, Germany
(Received 14 May 1969)

The multichannel relativistic Schrödinger equation is solved for the $\frac{3}{2}^+$ partial-wave amplitude with an energy-dependent potential obtained by computing the baryon exchange contribution to pseudoscalar-meson–baryon scattering. Since a cutoff parameter is not needed in our calculations, we use the coupling constant as an adjustable parameter. Thus we take $g^2/4\pi=38$ in order to obtain the $N^*(1236)$ at the correct experimental energy. The model yields the usual $\frac{3}{2}^+$ decuplet and predicts in addition the existence of a 27-dimensional $SU(3)$ representation [to which $P_{33}(1690)$, $P_{13}(1860)$, $Z_1(1900)$, and some higher Σ^*, Ξ^*, and Λ^* resonances could belong] as well as a second decuplet at much higher energies. Certain resonances ("exotic" ones with $I=2$, $Y=0$; $I=\frac{3}{2}$, $Y=-1$; and $I=1$, $Y=-2$) are very broad ($\approx$1000 MeV); others (the usual ones including the exotic $I=1$, $Y=2$ KN resonance) have a width $\leq$400 MeV. The dependence of the resonance spectrum on the breaking of $SU(3)$ symmetry as well as on the coupling constant and on the F/D ratio is discussed. A value of the F/D ratio of about 0.4 seems the best fit to experiments. The results are compared with the $\frac{3}{2}^+$ predictions of other models such as N/D calculations, quark model, strong-coupling theory, and $SU(3)''$ symmetry. In the two last-named models, a **27** appears also as a higher supermultiplet, which is forbidden in the quark model. Additional octets and $\bar{1}\bar{0}$ representations [predicted also by $SU(3)''$ and the quark model] are obtained as unphysical objects in our calculation.

I. INTRODUCTION

CONSIDERABLE study has been devoted to the theoretical understanding of the baryon spectrum. One of the main motivations for this is probably the large amount of existing experimental data as compared to the lack of understanding of strong-interaction physics. Among the techniques employed in the study of baryon spectroscopy particular attention has been devoted to the quark model.[1] In fact, its agreement with experiment is in general quite impressive. Nevertheless, usual arguments based on this model are nonrelativistic and qualitative. Quantitative calculations based on a relativistic quark model would certainly be of interest, but in addition to presenting the usual still unanswered questions (Where are the quarks?[2] Which form of statistics should be used? What is the form of the potential? Why should baryons be three-quark states?), it would also require the solution to a relativistic three-body problem. However, even if the above problem had been solved, the quark model cannot account for exotic states belonging to a **27** or higher $SU(3)$ representation, and which may be present experimentally.

In addition to the quark model and the usual procedure of assigning resonances to irreducible representations of internal symmetry groups such as $SU(3)$ and $SU(3)''$,[3,4] there are at least two additional main techniques which are frequently used to study the resonance spectrum.

The first consists in finding connections between masses, widths, and parities of groups of resonances.[5–7] The second type of technique, to which this paper as well as Ref. 8 belong, consists in performing dynamical calculations of the resonance spectrum under the assumption that its members are obtained as bound states or resonances of a subset of them.[8–13] This is carried to a logical extreme by the bootstrap philosophy in which one assumes that all particles are composite systems bound by forces obtained by the exchange of the particles themselves.[9]

Of course, in dynamical calculations of scattering amplitudes, the question arises as to which relativistic equation is to be used. These calculations should ideally employ the principles of relativistic invariance, unitarity, analyticity or causality, and crossing symmetry. It is customary to take into account the first three principles exactly and to ignore the last one.

* Supported in part by the Deutsche Forschungsgemeinschaft.
† Present address: Department of Physics, Purdue University, Lafayette, Ind. 47907.

[1] M. Gell-Mann, Phys. Rev. Letters **8**, 214 (1964); G. Zweig, CERN report No. 1964 (unpublished); R. Dalitz, in the *Proceedings of the Oxford International Conference on Elementary Particles, September, 1966* (Rutherford High-Energy Laboratory, Chilton, Berkshire, England, 1966); and in the *Proceedings of the Thirteenth International Conference on High-Energy Physics, Berkeley, California, 1966* (University of California Press, Berkeley, Calif., 1966).

[2] Yu. M. Antipov *et al.*, Phys. Letters **29B**, 245 (1969); T. Massam, CERN report No. 68-24, 1968 (unpublished).

[3] M. Gell-Mann, California Institute of Technology report No. CTSL-20, 1961 (unpublished); Phys. Rev. **125**, 1067 (1962); Y. Ne'eman, Nucl. Phys. **26**, 222 (1961).

[4] M. Y. Han and Y. Nambu, Phys. Rev. **139B**, 1006 (1965); O. W. Greenberg and C. A. Nelson, University of Maryland Technical Report No. 773, 1967 (unpublished); C. A. Nelson, University of Maryland Technical Report No. 868.

[5] B. Hamprecht and H. Kleinert, Fortschr. Physik **16**, 335 (1969).

[6] M. Sugawara, Phys. Rev. **172**, 1423 (1964).

[7] H. Genz, J. Katz, and S. Wagner, Nuovo Cimento (to be published).

[8] J. Katz, Nuovo Cimento **58A**, 125 (1968).

[9] G. F. Chew, Phys. Rev. **129**, 2363 (1963); G. F. Chew and F. E. Low, *ibid.* **101**, 1571 (1956).

[10] A. W. Martin and K. C Wali, Phys. Rev. **130**, 2455 (1963).

[11] K. C. Wali and R. L. Warnock, Phys. Rev. **135B**, 1358 (1964); R. C. Slansky, UCRL report No. 17450, 1967 (unpublished).

[12] H. W. Wyld, Jr., Phys. Rev. **155**, 1649 (1967).

[13] J. J. Brehm and G. L. Kane, Phys. Rev. **17**, 764 (1966).

By far the most common method used in calculating scattering amplitudes is the N/D method. Among the main disadvantages of this method are the Castillejo-Dalitz-Dyson (CDD) ambiguities[14] as well as the presence of overlapping cuts in dealing with multichannel problems, so that the N/D coupled system of integral equations cannot in general be solved exactly. Thus, most calculations involving this method use in one form or another the determinantal approximation, which essentially consists in solving the multichannel coupled system of integral equations to lowest order.

Another method which could in principle be used is the Bethe-Salpeter equation. One important practical disadvantage of this equation is that it involves, even after angular momentum decomposition, a two-dimensional integral equation, which is difficult to solve numerically. In addition it contains a relative energy variable and overlapping singularities which affect the compactness proof, for which one must perform a Wick rotation, which cannot be rigorously justified. A possible further disadvantage of this equation is that two-particle unitarity is satisfied only below the three-particle production threshold.

In this paper we study the $\frac{3}{2}^+$ baryon spectrum by solving the multichannel relativistic Schrödinger equation with a potential obtained by computing the baryon exchange contribution to pseudoscalar meson-baryon scattering. The model accounts for the usual $\frac{3}{2}^+$ decuplet (as in Ref. 8) and predicts the existence of a 27-dimensional $SU(3)$ representation [to which $\Delta(1690)$ could belong], as well as an additional $\frac{3}{2}^+$ decuplet at much higher energies. The dependence of the resonance spectrum on the breaking of $SU(3)$ symmetry as well as on the pion-nucleon coupling constant and the F/D ratio is discussed. The results of the calculation are compared with experiment in Sec. V. Finally, in Sec. VI we summarize our results and compare them with other theories.

II. RELATIVISTIC SCHRÖDINGER EQUATION

1. Discussion

Our calculational method consists in solving a multichannel relativistic Schrödinger equation. Starting from the usual decomposition of the Hamiltonian $H=H_0+V$, we obtain the integral equation for the T matrix, $T=V+VGT$, where V is the input potential and $G=(\sqrt{s}-H_0+i\epsilon)^{-1}$, with $\sqrt{s}$ being the total energy of the system and H_0 the free Hamiltonian. This equation can be assumed directly or obtained from the Bethe-Salpeter equation if one imposes two-particle unitarity by use of the Landau-Cutkosky rules and drops the extra term containing the energy denominator $(\sqrt{s}+E_q+\omega_q)^{-1}$ which corresponds to a 6-particle intermediate state (as discussed in Ref. 8).

[14] L. Castillejo, R. H. Dalitz, and F. J. Dyson, Phys. Rev. **101**, 453 (1956).

In order to make use of the relativistic Schrödinger equation in dynamical calculations, we must make sure that the principles of relativistic invariance, unitarity, and analyticity or causality are satisfied. To satisfy the first principle we use the relativistic expressions for the particle energies in H_0. It can then be shown that relativistic invariance is satisfied.[15,16] Two-particle unitarity also follows directly as shown in Sec. II 2. The causality properties of the equation were discussed by Coester.[17] He showed that such an equation obeys the principle of macrocausality, which states that the behavior of a system of particles should not be affected by the presence of other particles at a large distance from the system. It is worthwhile to remark at this point that from the physical point of view there is no *a priori* reason for microcausality to hold since only macrocausality can be experimentally proven. Thus some interest has been recently devoted to the study of macrocausal theories within different contexts such as, for example, that by Lee and Wick,[18] in which a macrocausal field theory is proposed in order to avoid some of the divergence problems which one frequently encounters in weak interactions.

Since the principles of relativistic invariance, unitarity, and analyticity or causality are satisfied, it follows that the relativistic Schrödinger equation is certainly an acceptable technique to be used in dynamical calculations, and may perhaps be a better method than other techniques based on the N/D method, since it includes iterations of the potential.

2. Two Particle Unitarity

Starting from the S matrix

$$S_{fi}=\delta_{fi}-(2\pi)^4 i\delta^{(4)}(p_f-p_i)\left(\frac{m_b m_d}{4a_0b_0c_0d_0}\right)^{1/2} M_{fi}, \quad (1)$$

and defining

$$M_{fi}=-4\pi\left(\frac{(a_0+b_0)(c_0+d_0)}{m_b m_d}\right)^{1/2} T_{fi}, \quad (2)$$

we obtain for the differential cross section

$$\frac{d\sigma}{d\Omega}=\frac{q_f}{q_i}|T_{fi}|^2, \quad (3)$$

where q_i and q_f denote the magnitude of the momenta in the c.m. frame in the initial and final states, respectively. Expanding

$$T=\sum_J (2J+1)d_{\lambda\mu}{}^J T^J, \quad (4)$$

[15] B. Bakamjian and L. H. Thomas, Phys. Rev. **92**, 1300 (1953).
[16] R. Fong and J. Sucher, J. Math. Phys. **5**, 456 (1963).
[17] F. Coester, Helv. Phys. Acta **38**, 7 (1965).
[18] T. D. Lee and G. C. Wick, Columbia University report No. 1969 (unpublished).

where $\lambda=\lambda_a-\lambda_b$, $\mu=\lambda_c-\lambda_d$, and $d_{\lambda\mu}(\theta)$ denotes the usual d function as given, for example, by Jacob and Wick,[19] the two-particle unitarity condition can be written in the form

$$\mathrm{Im}T_{\lambda_c\lambda_d;\lambda_a\lambda_b}{}^J=\sum_{ef}T_{\lambda_c\lambda_d;\lambda_e\lambda_f}{}^J q_{ef}T_{\lambda_e\lambda_f;\lambda_a\lambda_b}{}^\dagger, \quad (5)$$

where q_{ef} denotes the momentum of either particle in the two particle channel ef in the c.m. frame. Using matrix notation, and defining

$$T'^J=q_f{}^{1/2}T^J q_i{}^{1/2}, \quad (6)$$

we obtain

$$\frac{1}{T'^J}-\left(\frac{1}{T'^J}\right)^\dagger=2i, \quad (7)$$

where we have used the symmetry of the matrix T'^J, which follows from time-reversal invariance. Finally, we define the real symmetric matrix K'^J by

$$1/T'^J=(1/K'^J)-i. \quad (8)$$

The K'^J matrix is discussed, for example, by Dalitz and Tuan.[20]

The relativistic Schrödinger equation for K'^J is then

$$K'^J(q_f,q_i)=V'^J(q_f,q_i)-\frac{1}{\pi}P\int_{\Delta_m}^{\infty}V'^J(q_f,q)\times\frac{d(E_q+\omega_q)}{\sqrt{s}-E_q-\omega_q}K'^J(q,q_i), \quad (9)$$

where Δ_m is the lowest threshold.

3. Numerical Analysis

To solve the coupled system of integral equations (9), we make the transformation

$$\begin{aligned}(E_q+\omega_q)_i&=\alpha x_i/(1-x_i)+\Delta_i,\\ \sqrt{s}&=\alpha z_i/(1-z_i)+\Delta_i,\end{aligned} \quad (10)$$

where α is a scale factor chosen so as to make the integrand peak around the middle of the interval of integration, and where Δ_i is the threshold for the corresponding channel i.

To take care of the principal-value singularity in Eq. (9), we define

$$U'^J(x,z)=K'^J(x,z)\left[1-\frac{1}{\pi}\int_0^1\frac{dx'}{z-x'}K'^J(x',z)\right]^{-1}. \quad (11)$$

We can then rewrite Eq. (9) in the form

$$U'^J(x,z)=V'^J(x,z)-\frac{1}{\pi}\int_0^1\left[V'^J(x,x')\frac{dx'}{z-x'}\frac{1-z}{1-x'}-V'^J(x,z)\frac{dx'}{z-x'}\right]U'^J(x',z). \quad (12)$$

[19] M. Jacob and G. C. Wick, Ann. Phys. (N. Y.) 7, 404 (1959).
[20] R. Dalitz and S. F. Tuan, Ann. Phys. (N. Y.) 3, 307 (1960).

The above equation for $U'^J(x,z)$ is now solved by using Gaussian quadrature mesh points to convert it into a matrix equation which is solved by matrix inversion. Inverting Eq. (11) we then obtain $K'^J(x,z)$.

III. POTENTIAL USED IN CALCULATION

1. $SU(3)$ Contribution to Potential

Our calculation deals with the application of Eq. (9) to the problem of pseudoscalar meson-baryon scattering in the $P_{3/2}$ partial-wave amplitude. We choose the baryon exchange force as shown in Fig. 1 as our input potential and perform the off-shell extrapolation as discussed in Sec. III 2.

The following $SU(3)$-symmetric Lagrangian is used:

$$\begin{aligned}\mathfrak{L}_{\mathrm{int}}&=i\sqrt{2}g_{\pi N}\bar{B}_j{}^i\gamma_5[(1-2f)B_k{}^jP_i{}^k+B_i{}^kP_k{}^j]\\&=g_{\pi N}\boldsymbol{\pi}\cdot\bar{N}\boldsymbol{\tau}N+g_{\Lambda\pi\Sigma}(\boldsymbol{\pi}\cdot\bar{\Lambda}\boldsymbol{\Sigma}+\mathrm{H.c.})-ig_{\Sigma\pi\Sigma}\boldsymbol{\pi}\cdot(\boldsymbol{\Sigma}\times\boldsymbol{\Sigma})\\&\quad+g_{\Xi\pi\Xi}\boldsymbol{\pi}\cdot\bar{\Xi}\boldsymbol{\tau}\Xi+g_{\Lambda KN}(\bar{N}\Lambda K+\mathrm{H.c.})\\&\quad+g_{\Sigma KN}(\mathbf{N}\boldsymbol{\tau}\cdot\boldsymbol{\Sigma}K+\mathrm{H.c.})+g_{\Lambda K\Xi}(\bar{\Xi}\Lambda K^c+\mathrm{H.c.})\\&\quad+g_{\Sigma K\Xi}(\boldsymbol{\Xi}\boldsymbol{\tau}\cdot\boldsymbol{\Sigma}K^c+\mathrm{H.c.})+g_{N\eta N}\bar{N}N\eta\\&\qquad+g_{\Lambda\eta\Lambda}\eta\bar{\Lambda}\Lambda+g_{\Sigma\eta\Sigma}\eta\bar{\Sigma}\cdot\Sigma+g_{\Xi\eta\Xi}\eta\bar{\Xi}\Xi. \quad (13)\end{aligned}$$

In the above expression, $g_{\pi N}$ denotes the pion-nucleon coupling constant (with the physical value $g_{\pi N}{}^2/4\pi=14.6$), f denotes the F/D ratio (physical value ≈ 0.33), $B_j{}^i$ and $P_j{}^i$ are the baryon and pseudoscalar meson octets, respectively, and in addition we have defined

$$\begin{aligned}g_{\Lambda\pi\Sigma}&=(2/\sqrt{3})(1-f)g,\\ g_{\Sigma\Lambda\Sigma}&=2fg,\\ g_{\Xi\pi\Xi}&=(1-2f)g,\\ g_{\Lambda KN}&=-(1/\sqrt{3})(1+2f)g,\\ g_{\Sigma KN}&=(1-2f)g,\\ g_{\Lambda K\Xi}&=-(1/\sqrt{3})(1-4f)g,\\ g_{\Sigma K\Xi}&=g,\\ g_{N\eta N}&=-(1/\sqrt{3})(1-4f)g,\\ g_{\Lambda\eta\Lambda}&=-(2/\sqrt{3})(1-f)g,\\ g_{\Sigma\eta\Sigma}&=(2/\sqrt{3})(1-f)g,\end{aligned} \quad (14)$$

and

$$g_{\Xi\eta\Xi}=-(1/\sqrt{3})(1-2f)g,$$

where

$$g=g_{\pi N}.$$

The multichannel relativistic Schrödinger equation is then solved with the above potential, which is equivalent to imposing two-particle unitarity on the infinite sum of ladder diagrams shown in Fig. 2 and dropping the extra term corresponding to the six-particle intermediate states. The bound states and resonance spec-

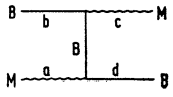

FIG. 1. Baryon-exchange contribution to the driving force.

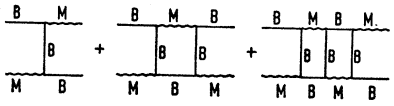

FIG. 2. Infinite sum of ladder diagrams considered in the calculation.

trum are then studied as well as their dependence on the parameters f and g and the symmetry breaking.

In our calculation, $SU(3)$ symmetry is assumed for the coupling constants. However, the input masses are in general assumed to be unequal within each $SU(3)$ representation. Either the physical masses are taken, or in order to study the effect of symmetry breaking, the masses are obtained from the expression

$$M=M_0'\{1+x[a'Y+b'(I(I+1)-\tfrac{1}{4}Y^2)]\} \quad (15)$$

in the case of baryons, and

$$M^2=M_0''^2\{1+xb''[I(I+1)-\tfrac{1}{4}Y^2]\} \quad (16)$$

in the case of mesons. The $SU(3)$-symmetry-breaking effects are then discussed by studying the dependence of the results on the parameter x so introduced. Note that in the above $x=0$ corresponds to perfect symmetry, while $x=1$ corresponds to fully broken symmetry, since the parameters M_0, M_0', a', b', and b'' are to be determined by the fit to the physical masses in the case of $x=1$.

2. Momentum Dependence of Potential

We write in the usual way

$$M_{fi}=\bar{u}(\mathbf{d})[-A+\tfrac{1}{2}i\gamma(a+c)B]u(\mathbf{b}),$$

where a, c, b, and d denote the energy-momentum of the pseudoscalar mesons and of the baryons respectively. Defining[21]

$$\begin{aligned}X&=[-A-\tfrac{1}{2}B(a_0+b_0+c_0+d_0-m_b-m_d)],\\ Y&=[A-\tfrac{1}{2}B(a_0+b_0+c_0+d_0+m_b+m_d)]\\ &\quad\times\left(\frac{(b_0-m_b)(d_0-m_d)}{(b_0+m_b)(d_0+m_d)}\right)^{1/2},\end{aligned} \quad (17)$$

and

$$\begin{pmatrix}X_l\\Y_l\end{pmatrix}=\frac{1}{2}\int_{-1}^{+1}dx\begin{pmatrix}X\\Y\end{pmatrix}P_l(x), \quad (18)$$

we obtain

$$V_l'^{\pm}=-\frac{1}{4\pi}\left[\frac{(b_0+m_b)(d_0+m_d)}{(b_0+a_0)(d_0+c_0)}\right]^{1/2}\times(|\mathbf{b}||\mathbf{d}|)^{1/2}[X_l+Y_{l\pm1}]. \quad (19)$$

[21] In our calculation we shall make the replacement $a_0+b_0+c_0+d_0\to 2\sqrt{s}$, since only the on-shell potential is known. In this way we avoid a cutoff and obtain an energy-dependent potential. Possible other ways of performing the off-shell extrapolation have already been discussed in Ref. 8.

The contribution due to the baryon exchange force as shown in Fig. 1 is then

$$\begin{aligned}A=&-[m_e-\tfrac{1}{2}(m_b+m_d)]\\ &\times\{[(b+d)^2-\tfrac{1}{4}(b_0-a_0-c_0+d_0)^2+m_e^2]\}^{-1}\end{aligned} \quad (20)$$

and

$$B=-\{[(b+d)^2-\tfrac{1}{4}(b_0-a_0-c_0+d_0)^2+m_e^2]\}^{-1}, \quad (21)$$

where the mass of the baryon being exchanged is denoted by m_e. Thus A_l and B_l may be written as

$$A_l=[m_e-\tfrac{1}{2}(m_b+m_d)][(-1)^{l+1}/2|\mathbf{b}||\mathbf{d}|]Q_l(z) \quad (22)$$

and

$$B_l=[(-1)^{l+1}/2|\mathbf{b}||\mathbf{d}|]Q_l(z), \quad (23)$$

with

$$z=\frac{|\mathbf{b}|^2+|\mathbf{d}|^2-\tfrac{1}{4}(a_0-b_0-d_0+c_0)^2+m_e^2}{2|\mathbf{b}||\mathbf{d}|}. \quad (24)$$

Once the momentum dependence of the potential is calculated, the total potential is obtained by multiplying the above expression by the corresponding $SU(3)$ dependence.

3. $SU(3)$ Dependence of Potential

By use of the BPB interaction Lagrangian given in Eq. (13), we obtain as a result of the contraction for the process in question the expression

$$\begin{aligned}2g_{\pi N}^2\{&[(1-2f)B_k{}^j(P_i^\dagger)^k+B_i{}^k(P_k^\dagger)^j]\\ &\times[(1-2f)\bar{B}_j{}^lP_l{}^i+\bar{B}_l{}^iP_j{}^l]\\ &-\tfrac{1}{3}[(1-2f)B_k{}^j(P_j^\dagger)^k+B_j{}^k(P_k^\dagger)^j]\\ &\times[(1-2f)\bar{B}_i{}^lP_l{}^i+\bar{B}_l{}^iP_i{}^l]\},\end{aligned} \quad (25)$$

from which we obtain

$$\begin{aligned}[&\tfrac{4}{3}(4f^2-2f+1)|T\rangle\langle T|-2(4f^2-2f+1)|\Theta_s\rangle\langle\Theta_s|\\ &+\tfrac{2}{3}(4f^2+10f-5)|\Theta_a\rangle\langle\Theta_a|\\ &-(8/3)(2f^2-f-1)|D\rangle\langle D|\\ &+(8/3)(4f^2-5f+1)|\bar{D}\rangle\langle\bar{D}|\\ &-\tfrac{4}{3}(4f^2+10f-5)|S\rangle\langle S|]g_{\pi N}^2.\end{aligned} \quad (26)$$

In the above expression, $|S\rangle$, $|\Theta_s\rangle$, $|\Theta_a\rangle$, $|D\rangle$, $|\bar{D}\rangle$, and $|T\rangle$ denote the normalized scalar, symmetrical octet, and antisymmetrical octet, **10**, $\bar{\mathbf{10}}$, and **27**, respectively.

The contribution to the different isotopic spin, hypercharge states is easily computed in the case of perfect symmetry once we have the crossing matrix given above by using, for example, de Swart's table.

In the case of broken $SU(3)$ symmetry the above procedure can also be used, except in the case of Λ and Σ exchange, where it is more convenient to calculate the

crossing matrix directly by multiplying the relevant $SU(3)$ coupling constants by the isotopic spin crossing matrix, calculated in the standard fashion.

We next list for each relevant hypercharge, isospin state the $SU(3)$ crossing coefficients which we use in our calculation as a matrix whose (i,j) element represents the crossing coefficient for scattering from channel i to channel j, and where the symbol in parentheses next to each crossing coefficient represents the particles being exchanged. Because of symmetry we need only to list half of the off-diagonal terms.

$$I=0,\ Y=2;\ Z_0$$

$$\begin{array}{c} \\ KN \end{array}\begin{array}{c} KN \\ \left[\begin{array}{c} -\frac{1}{3}(1+4f+4f^2)\ (\Lambda) \\ +3(1-4f+4f^2)\ (\Sigma) \end{array}\right] g^2 \end{array}$$

$$I=1,\ Y=2;\ Z_1$$

$$\begin{array}{c} \\ KN \end{array}\begin{array}{c} KN \\ \left[\begin{array}{c} \frac{1}{3}(1+4f+4f^2)\ (\Lambda) \\ +\frac{1}{3}(1-4f+4f^2)\ (\Sigma) \end{array}\right] g^2 \end{array}$$

$$I=\tfrac{1}{2},\ Y=1;\ N$$

$$\begin{array}{c} \\ \pi N \\ \eta N \\ K\Lambda \\ K\Sigma \end{array}\begin{array}{c} \begin{array}{cccc} \pi N & \eta N & K\Lambda & K\Sigma \end{array} \\ \left[\begin{array}{cccc} -1\ (N) & (1-4f)\ (N) & -2(1-3f+2f^2)\ (\Sigma) & \frac{2}{3}(1+f-2f^2)\ (\Lambda) \\ & & & -2(2f-4f^2)\ (\Sigma) \\ & \frac{1}{3}(1-8f+16f^2)\ (N) & \frac{2}{3}(1+f-2f^2)\ (\Lambda) & 2(1-3f+2f^2)\ (\Sigma) \\ & & \frac{1}{3}(1-8f+16f^2)\ (\Xi) & -(1-4f)\ (\Xi) \\ & & & -1\ (\Xi) \end{array}\right] g^2 \end{array}$$

$$I=\tfrac{3}{2},\ Y=1;\ \Delta$$

$$\begin{array}{c} \\ \pi N \\ K\Sigma \end{array}\begin{array}{c} \begin{array}{cc} \pi N & K\Sigma \end{array} \\ \left[\begin{array}{cc} 2\ (N) & -\frac{2}{3}(1+f-2f^2)\ (\Lambda) \\ & -2(f-2f^2)\ (\Sigma) \\ & 2\ (\Xi) \end{array}\right] g^2 \end{array}$$

$$I=0,\ Y=0;\ \Lambda^*$$

$$\begin{array}{c} \\ \pi\Sigma \\ \bar{K}N \\ \eta\Lambda \\ K\Xi \end{array}\begin{array}{c} \begin{array}{cccc} \pi\Sigma & \bar{K}N & \eta\Lambda & K\Xi \end{array} \\ \left[\begin{array}{cccc} \frac{4}{3}(1-f)^2\ (\Lambda) & -(\sqrt{6})(1-2f)\ (N) & (\frac{4}{3}\sqrt{3})(1-f)^2\ (\Sigma) & (\sqrt{6})(1-2f)\ (\Xi) \\ -8f^2\ (\Sigma) & & & \\ & 0 & (\frac{1}{3}\sqrt{2})(1-2f-8f^2)\ (N) & -\frac{1}{3}(1-2f-8f^2)\ (\Lambda) \\ & & & -3(1-2f)\ (\Sigma) \\ & & \frac{4}{3}(1-f)^2\ (\Lambda) & -(\frac{1}{3}\sqrt{2})(1-2f-8f^2)\ (\Xi) \\ & & & 0 \end{array}\right] g^2 \end{array}$$

$$I=1,\ Y=0;\ \Sigma^*$$

$$\begin{array}{c} \\ \pi\Lambda \\ \pi\Sigma \\ \bar{K}N \\ \eta\Sigma \\ K\Xi \end{array}\begin{array}{c} \begin{array}{ccccc} \pi\Lambda & \pi\Sigma & \bar{K}N & \eta\Sigma & K\Xi \end{array} \\ \left[\begin{array}{ccccc} \frac{4}{3}(1-f)^2\ (\Sigma) & 4(\sqrt{\frac{2}{3}})(f-f^2)\ (\Sigma) & (\sqrt{\frac{2}{3}})(1+2f)\ (N) & -\frac{4}{3}(1-f)^2\ (\Lambda) & (\sqrt{\frac{2}{3}})(1-6f+8f^2)\ (\Xi) \\ & -\frac{4}{3}(1-f)^2\ (\Lambda) & 2(1-2f)\ (N) & -4(\sqrt{\frac{2}{3}})(f-f^2)\ (\Sigma) & -2(1-2f)\ (\Xi) \\ & +4f^2\ (\Sigma) & & & \\ & & 0 & (\sqrt{\frac{2}{3}})(1-6f+8f^2)\ (N) & -\frac{1}{3}(1-2f+8f^2)\ (\Lambda) \\ & & & & -(1-2f)\ (\Sigma) \\ & & & \frac{4}{3}(1-f)^2\ (\Sigma) & \frac{2}{3}(1+2f)\ (\Xi) \\ & & & & 0 \end{array}\right] g^2 \end{array}$$

$$I=2,\ Y=0$$

$$\begin{array}{c} \\ \pi\Sigma \end{array}\begin{array}{c} \pi\Sigma \\ \left[\begin{array}{c} \frac{4}{3}(1-f)^2\ (\Lambda) \\ +4f^2\ (\Sigma) \end{array}\right] g^2 \end{array}$$

$$I=\tfrac{1}{2},\ Y=-1;\ \Xi^*$$

$$\begin{array}{c} \\ \pi\Xi \\ \bar{K}\Lambda \\ \bar{K}\Sigma \\ \eta\Xi \end{array}\begin{array}{c} \begin{array}{cccc} \pi\Xi & \bar{K}\Lambda & \bar{K}\Sigma & \eta\Xi \end{array} \\ \begin{bmatrix} -(1-4f+4f^2)\ (\Xi) & 2(1-f)\ (\Sigma) & \tfrac{2}{3}(1-5f+4f^2)\ (\Lambda) & -(1-4f^2)\ (\Xi) \\ & \tfrac{1}{3}(1+4f+4f^2)\ (N) & +4f\ (\Sigma) & \\ & & (1-4f^2)\ (N) & \tfrac{2}{3}(1-5f+4f^2)\ (\Xi) \\ & & -(1-4f+4f^2)\ (N) & -2(1-f)\ (\Sigma) \\ & & & \tfrac{1}{3}(1+4f+4f^2)\ (\Xi) \end{bmatrix} \end{array} g^2$$

$$I=\tfrac{3}{2},\ Y=-1$$

$$\begin{array}{c} \\ \pi\Xi \\ \bar{K}\Sigma \end{array}\begin{array}{c} \begin{array}{cc} \pi\Xi & \bar{K}\Sigma \end{array} \\ \begin{bmatrix} 2(1-4f+4f^2)\ (\Xi) & -\tfrac{2}{3}(1-5f+4f^2)\ (\Lambda) \\ & +2f\ (\Sigma) \\ & 2(1-4f+4f^2)\ (N) \end{bmatrix} \end{array} g^2$$

$$I=0,\ Y=-2;\ \Omega^-$$

$$\begin{array}{c} \\ \bar{K}\Xi \end{array}\begin{array}{c} \begin{array}{c} \bar{K}\Xi \end{array} \\ \begin{bmatrix} -\tfrac{1}{3}(1-8f+16f^2)\ (\Lambda) \\ +3\ (\Sigma) \end{bmatrix} \end{array} g^2$$

$$I=1,\ Y=-2$$

$$\begin{array}{c} \\ \bar{K}\Xi \end{array}\begin{array}{c} \begin{array}{c} \bar{K}\Xi \end{array} \\ \begin{bmatrix} \tfrac{1}{3}(1-8f+16f^2)\ (\Lambda) \\ +1\ (\Sigma) \end{bmatrix} \end{array} g^2.$$

IV. RESULTS OF CALCULATION

1. Lower $\frac{3}{2}^+$ Decuplet

The lower $\frac{3}{2}^+$ decuplet has already been discussed in Ref. 8 for physical input masses and an F/D ratio of 0.33. The coupling constant was chosen to be $g^2/4\pi=38$ in order to fit the resonance energy of the $\Delta(1236)$. (See the discussion on the $g^2/4\pi$ value in Sec. V.)

In this paper we first wish to discuss the dependence of the $\frac{3}{2}^+$ decuplet on the F/D ratio. In Table I the bound state and resonance energies for the members of the decuplet are given for different values of the F/D ratio, namely, $f=0.25$, 0.33, and 0.5. Note that similar to the N/D results,[11] this model exhibits a very weak dependence on the F/D ratio, as the potential strengths for the decuplet suggest.

Next we wish to discuss the effect of $SU(3)$ symmetry breaking. Before doing this we wish to note that (see Fig. 3 and in Ref. 8, Table I, Col. 3) when physical input masses are used in the calculation, the decuplet masses are obtained in qualitative agreement with the equal-spacing rule. The average mass difference between consecutive members is then obtained to be about 185 MeV, and one obtains an increase of this mass difference with increasing hypercharge. Similar results were obtained using the N/D method,[11] although in that model there is an even stronger hypercharge dependence. In order to

TABLE I. The $\frac{3}{2}^+$ decuplet. Calculated resonance and bound state energies of the lower $\frac{3}{2}^+$ decuplet are given in MeV for values of the F/D ratio $f=0.33$, 0.25, and 0.5 for a coupling constant $g^2/4\pi=38$. The last three lines contain the mass differences between consecutive members of the decuplet. Experimentally the equal spacing rule is fulfilled and these mass differences are about 150 MeV.

I	Y	Symbol	$f=0.33$	$f=0.25$	$f=0.5$
$\frac{3}{2}$	1	Δ	1236	1235	1238
1	0	Σ^*	1444	1443	1448
$\frac{1}{2}$	-1	Ξ^*	1627	1627	1633
0	-2	Ω^-	1801	1790	1840
	Ω^- appears as a		bound state	bound state	resonance
m_{Σ^*}	$-m_{\Delta^*}$		208	208	210
m_{Ξ^*}	$-m_{\Sigma^*}$		185	184	185
m_Ω	$-m_{\Xi^*}$		172	163	207

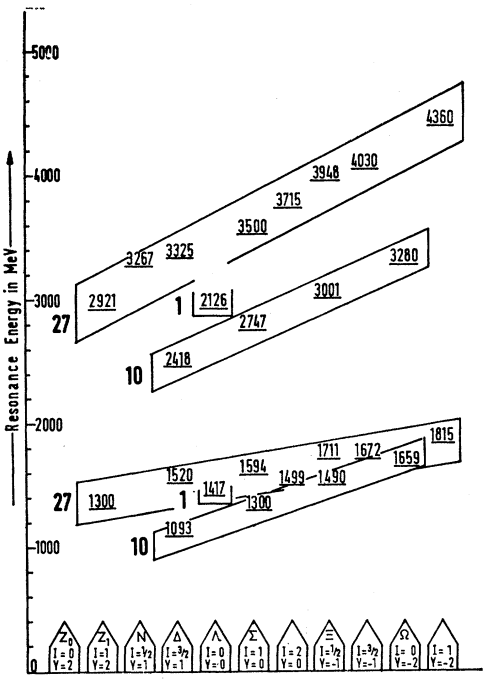

FIG. 3. Calculated $\frac{3}{2}^+$ baryon spectrum for $g^2/4\pi=38$ and F/D ratio $f=0.33$. Resonances are represented as lines in the energy scale. Above each line the resonance or bound-state energy is given in MeV. Positions of "antiresonances" (i.e., the energies at which one of the eigenphases passes 90° when descending) are indicated by dashed lines. The widths are given (in MeV) below the lines.

study the symmetry-breaking effects, we proceed as has been previously done in the N/D calculations.[11] That is, the validity of Eqs. (14) and (15) is assumed. These equations are obtained from the Gell-Mann–Okubo[22] mass formula upon introduction of a parameter x which may vary between 0 and 1. The case $x=0$ corresponds to the perfect $SU(3)$ limit, while the case $x=1$ corresponds to fully broken $SU(3)$ symmetry. The parameters of Eqs. (15) and (16) are determined to be

$$\begin{aligned} &M_0'=m_\Lambda, \quad a'=-195.5/m_\Lambda, \quad b'=39/m_\Lambda, \\ &M_0''=m_\eta, \qquad\qquad\qquad b''=-141179/m_\eta^2. \end{aligned} \tag{27}$$

The values of the above constants were obtained using physical masses for m_Λ, m_N, m_Σ, m_η, and m_π. However, the values $m_\Xi=1330$ MeV (instead of 1318 MeV) and $m_K=m_{\bar{K}}=480$ MeV (instead of 496 MeV) were used in order to require the Gell-Mann–Okubo mass formula to be exactly valid. The x dependence is shown in Fig. 4. It is worthwhile to note that the results for $x=1$, i.e., fully broken symmetry, deviate by less than 1 MeV from the case in which all masses are taken to be physical. For $x=0$, i.e., perfect symmetry, all decuplet members appear (for a coupling constant $g^2/4\pi=38$) as bound states at an energy of about 1565 MeV.

The dependence of the decuplet energies on the coupling constant was also studied. The results are shown in Fig. 5, in which the resonance and bound-state energies are plotted as functions of $(g^2/4\pi)^{-1}$. From this figure we see that this dependence is nearly linear in the range $0\leq(g^2/4\pi)^{-1}\leq 0.1$.[23–26] Notice that Fig. 5 shows

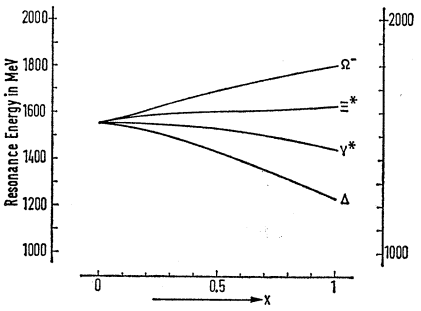

FIG. 4. $SU(3)$ symmetry breaking of the lower $\frac{3}{2}^+$ decuplet. The dependence of the resonance or bound-state energies of the members of the usual $\frac{3}{2}^+$ decuplet on the $SU(3)$ symmetry-breaking parameter x [as introduced in Eqs. (15), (16), and (27)] is given. $x=0$ corresponds to perfect $SU(3)$ symmetry, while for $x=1$ the symmetry is fully broken so that the Gell-Mann–Okubo mass formula holds for the input particles with about the same masses as the physical ones.

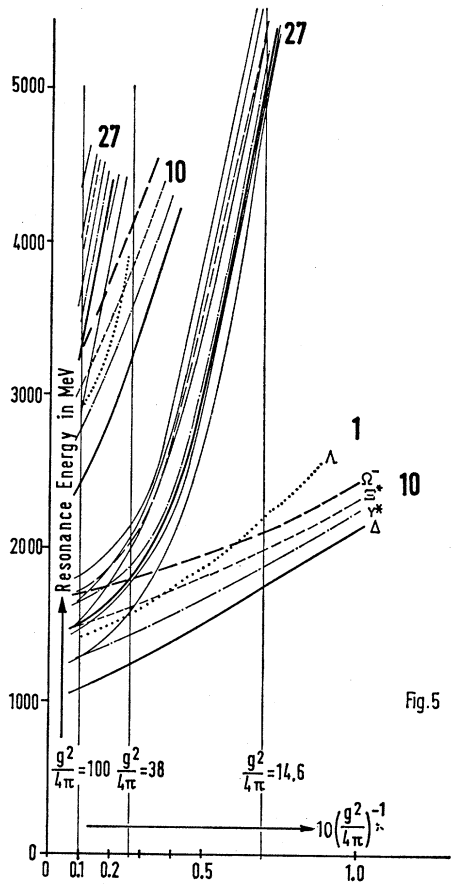

Fig.5

FIG. 5. Reciprocal g^2 dependence of the $\frac{3}{2}^+$ resonance spectrum for the F/D ratio $f=0.33$. The dependence of the resonance and bound-state energies of the $\frac{3}{2}^+$ spectrum on $(g^2/4\pi)^{-1}$ is given. The Δ states are represented by thick solid lines, the Σ^* states by dot-dashed lines, the Ξ^* states by short dashed lines, the Ω^- states by long dashed lines, and the Λ^* states by dotted lines. All other states are represented by thin solid lines.

that the equal-spacing rule is better fulfilled the larger the coupling constant, since for lower values of $g^2/4\pi$ the Y^* and Ξ^* resonances come closer and closer together. Let us also note that for $g^2/4\pi=14.6$ the equal-spacing rule is less well fulfilled than for $g^2/4\pi=38$, although the average mass splitting then becomes about the same as the experimental one.

2. 27 Supermultiplet and Singlet

The model predicts a 27-dimensional $SU(3)$ representation at energies of about 400 MeV above the usual

[22] M. Gell-Mann, California Institute of Technology Synchrotron Laboratory report No. CTSL-20, 1961 (unpublished); S. Okubo, Progr. Theoret. Phys. (Kyoto) **27**, 949 (1962).

[23] A proportionality of the resonance energies on $(g^2/4\pi)^{-1}$ follows from Wentzel's strong-coupling approach (Ref. 24) if one only keeps the lowest term in an expansion in terms of $(g^2/4\pi)^{-1}$. In numerical applications of this theory (Ref. 25) it was usually assumed that these lowest-order terms should already give the main contribution, even for the physical coupling constant $g^2/4\pi=14.6$. Our model seems to be in agreement with this assumption. As will become clear in the rest of this paper, further analogies between the model here considered and the $SU(3)$ modification of strong-coupling theory (Ref. 26) are the weak dependence on the F/D ratio and the occurrence of 10- and 27-dimensional $SU(3)$ representations in case of spin $\frac{3}{2}^+$. Among the main differences between both models is the fact that in the strong-coupling limit these resonances become stable. An additional difference between them is that our model predicts a second decuplet and could never predict 35-dimensional supermultiplets.

[24] G. Wentzel, Helv. Phys. Acta **13**, 169 (1940); **16**, 551 (1943).

[25] F. Villars, Helv. Phys. Acta **19**, 323 (1946); S. Wagner, Phys. Rev. **177**, 2278 (1969); S. Wagner and P. Winiger, Helv. Phys. Acta **42**, 51 (1969).

[26] C. Goebel, Phys. Rev. Letters **16**, 1130 (1966); C. Dullemond and J. M. van der Linden, Ann. Phys. (N. Y.) **41**, 372 (1967).

decuplet, together with a singlet which appears at lower energies. The resonance energies are given in Figs. 3 and 5 while the eigenphases and Argand dia-

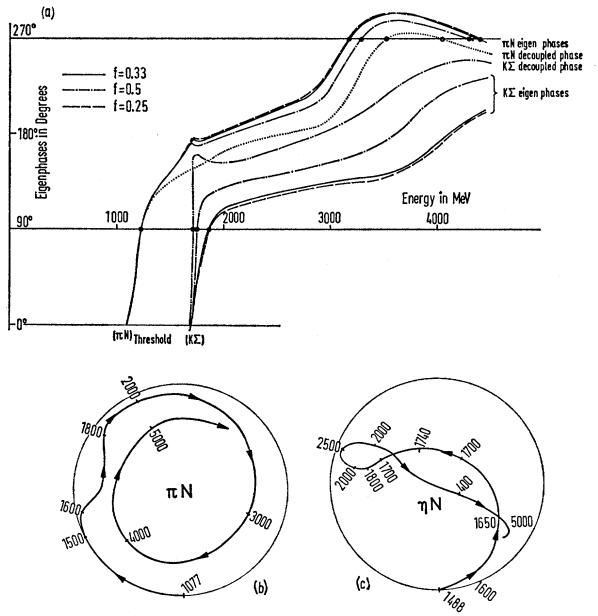

FIG. 6. Eigenphases and Argand diagrams for the $\frac{3}{2}^+$ Δ State $I=\frac{3}{2}$, $Y=1$ for $g^2/4\pi=38$. (a) Eigenphases for the F/D ratios $f=0.33$ (solid lines), $f=0.25$ (dashed lines), and $f=0.5$ (dot-dashed lines). In addition the decoupled πN (dotted line) and $K\Sigma$ (two dot-dashed line) phase shifts are given. Positions of resonances are marked by closed circles and of "antiresonances" by open circles; (b) and (c) Argand diagrams for the πN and $K\Sigma$ channels of the Δ state for $g^2/4\pi=38$ and $f=0.33$.

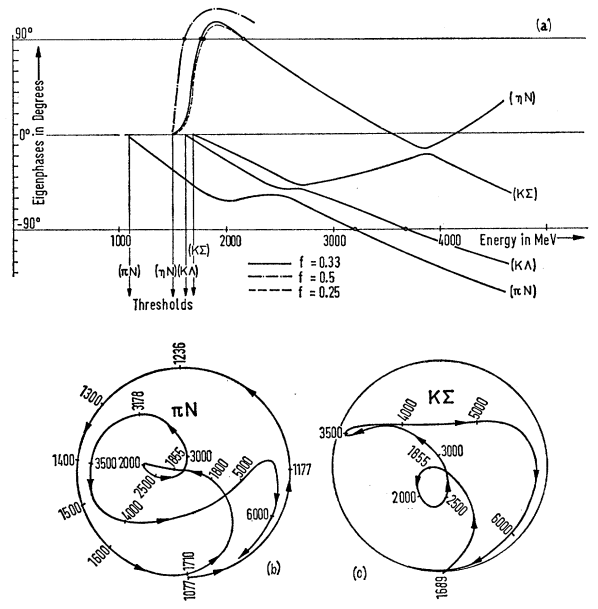

FIG. 7. Eigenphases and Argand diagrams for the $\frac{3}{2}^+$ N state $I=\frac{1}{2}$, $Y=1$ for $g^2/4\pi=38$. (a) Eigenphases for the F/D ratio $f=0.33$ (solid lines), $f=0.25$ (dashed lines), and $f=0.5$ dot-dashed lines; (b) and (c) Argand diagrams for the πN and ηN channels of the N state for $g^2/4\pi=38$ and $f=0.33$.

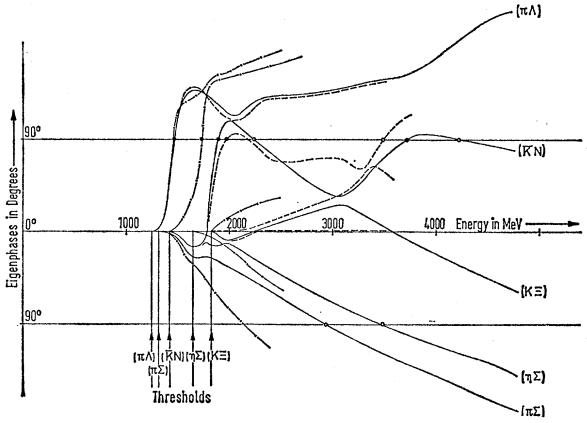

FIG. 8. Eigenphases for the $\frac{3}{2}^+$ state $I=1$, $Y=0$ for $g^2/4\pi=38$ and $f=0.33$, 0.25, and 0.5.

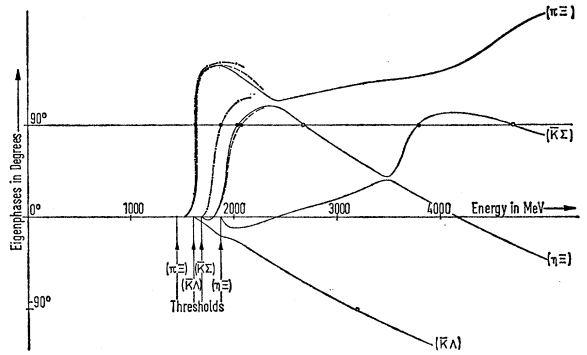

FIG. 9. Eigenphases for the $\frac{3}{2}^+$ state $I=\frac{1}{2}$, $Y=-1$ for $g^2/4\pi=38$ and $f=0.33$, 0.25, and 0.5.

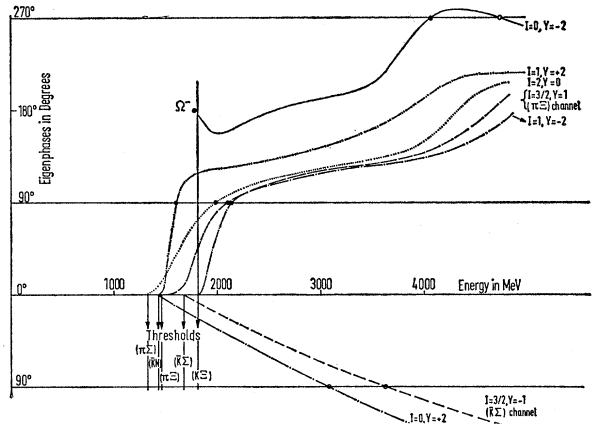

FIG. 10. Eigenphases for the $\frac{3}{2}^+$ exotic states and Ω^- for $g^2/4\pi=38$ and $f=0.33$. Solid line: $I=0$, $Y=-2$ (decuplet Ω^- state with bound-state position marked as closed circle). Dot-dashed line: $I=0$, $Y=+2$ (belonging to $\overline{10}$ representation). Other lines are as indicated on figure; they are exotic states belonging to a 27-dimensional $SU(3)$ representation.

grams are given in Figs. 6–12. Note that all states which are common to both the 10- and the 27-dimensional representation, namely, Δ, Σ^*, and Ξ^*, resonate in different channels in each of these two cases.

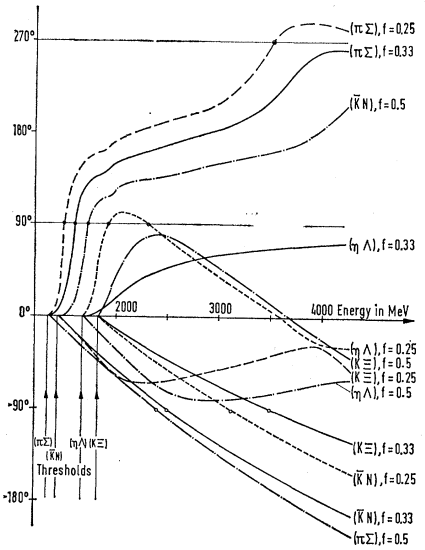

FIG. 11. Eigenphases for the $\frac{3}{2}$ Λ^* state $I=0$, $Y=0$ for $g^2/4\pi=38$ and $f=0.33$, 0.25, and 0.5.

While the first Δ resonance $\Delta(1236)$ (which is a member of a **10**) is a purely elastic πN resonance, the second Δ resonance (which is a member of a **27**) appears at an energy of about 1852 MeV as a predominantly $K\Sigma$ resonance. The width of this resonance is about 300 MeV. This is in qualtiative agreement with experiment (see Sec. V). Figure 6(a) shows the eigenphases of the Δ state when both the πN and $K\Sigma$ channel are taken into account and the phase shifts when only one of them is considered. Notice that in the case of $\Delta(1236)$, the decoupled πN phase shift is very close to the corresponding eigenphase when both channels are included, i.e., $K\Sigma$ effects are unimportant in the study of the $\Delta(1236)$ resonance. In the case of the second resonance $\Delta(1690)$, the $K\Sigma$ eigenphase goes through 90° while the πN eigenphase does not. If we uncouple the channels, we note that the πN phase shift does not exhibit a resonance behavior in addition to that at $\Delta(1236)$ (except at much higher energies where the second decuplet resonance occurs, which will be discussed in Sec. IV 3). Note also that the decoupled $K\Sigma$ phase shift is very close to the corresponding eigenphase in the resonance region. This implies that the second Δ resonance is mainly a $K\Sigma$ resonance.[27]

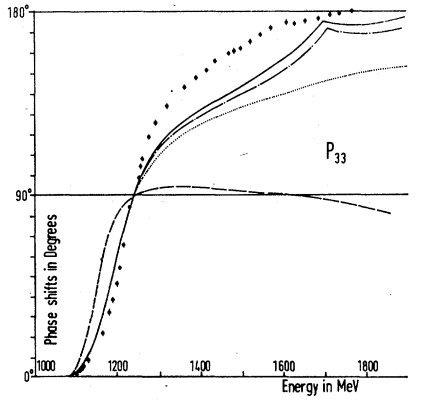

FIG. 12. Experimental and calculated P_{33} phase shifts. The solid lines (dot-dash lines) indicate the calculated eigenphase shifts for $g^2/4\pi=38$ and $f=0.33$ (for $g^2/4\pi=38$ and $f=0.5$). The dotted lines indicate the decoupled πN phase shifts for $g^2/4\pi=38$. The dashed lines indicate the calculated phase shifts using the Bethe-Salpeter equation with Padé approximants for πN scattering as given in Ref. 33. The experimental CERN phase shifts as given in Ref. 28 are explicitly exhibited in the graph by the error bars.

The eigenphases and Argand diagrams corresponding to the other isospin, hypercharge states are given in Figs. 9–11. Note in passing that according to a theorem derived by Wigner, eigenphases do not cross so that the resonating channel may be recognized unambiguously also for higher energies (see Figs. 6–11).

Figures 9–11 show that in addition to the second Δ there are two exotic **27** kaon resonances, namely, the $I=1$, $Y=+2$ Kp resonance at an energy of about 1609 MeV, and the $I=1$, $Y=-2$ $\bar{K}\Xi$ resonance at about 2140 MeV. There are two exotic pion resonances, namely, the one-channel $I=2$, $Y=0$ $\pi\Sigma$ resonance and the two-channel $I=\frac{3}{2}$, $Y=-1$ resonance, for which the $\pi\Xi$ eigenphase goes through 90°. The resonances in the N, Σ^*, and Ξ^* states (which are usually fitted into an octet) resonate in the channels (ηN), $(\bar{K}N)$, and $(\bar{K}\Sigma)$, respectively. The Λ^* is a special case which shall be considered separately. The resonance energies for the members of the **27** (as well as the two decuplets) are given in Fig. 3 for $g^2/4\pi=38$ and $f=0.33$, in Table II for $f=0.33$ as well as for other F/D values, and in Fig. 13 for $g^2/4\pi=100$ and $f=0.33$. All the resonances mentioned above fill a complete **27** supermultiplet. In addition note that there is no resonance behavior in the $I=0$, $Y=+2$ state, so that in our model a $\frac{3}{2}^+$ super-

TABLE II. The **27** supermultiplet. Resonance energies in MeV for members of the **27** and singlet $SU(3)$ representations are given for F/D values $f=0.33$, 0.25, and 0.5 for a coupling constant $g^2/4\pi=38$. The widths are given in parentheses. In case of Λ^* the results are given in the upper or lower line according as to whether the singlet or **27** $I=0$, $Y=0$ state is the dominant one.

I	Y	Symbol	$f=0.33$	$f=0.25$	$f=0.5$
1	2	Z_1	1609 (336)	1631 (382)	1502 (83)
$\frac{1}{2}$	1	N	1755 (385)	1776 (245)	1606 (250)
$\frac{3}{2}$	1	Δ	1852 (337)	1871 (457)	1756 (104)
0	0	Λ^*	1597 (150)	1493 (89)	
				1920 (720)	1710 (290)
1	0	Σ^*	1879 (317)	1960 (716)	1729 (127)
2	0		1990 (1440)	2079 (1635)	1776 (955)
$\frac{1}{2}$	−1	Ξ^*	2036 (716)	2064 (716)	1881 (294)
$\frac{3}{2}$	−1		2083 (1430)	2108 (1430)	1885 (880)
1	−2		2140 (955)	2150 (1146)	1987 (317)

[27] Thus our model suggests that in order to understand the baryon spectrum using the techniques applied in Refs. 6 and 7, it is helpful to include $SU(3)$ effects explicitly.

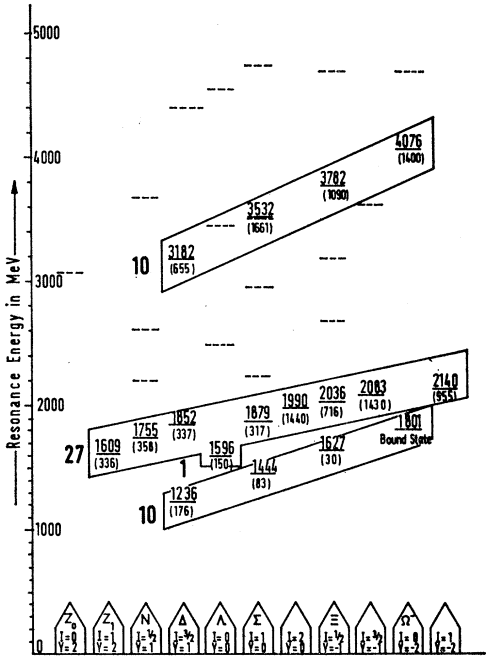

FIG. 13. Calculated $\frac{3}{2}^+$ baryon spectrum for $g^2/4\pi=100$ and an F/D value $f=0.33$.

multiplet belonging to a $\bar{1}\bar{0}$ representation does not occur.

The widths of the members of the **27** are also given in parentheses in Fig. 3 and also in Table II. Note that those exotic resonances which have not yet been observed experimentally, namely, the $I=2$, $Y=0$; $I=\frac{3}{2}$, $Y=-1$, and $I=1$, $Y=-2$ states appear in our model with extremely large widths. However, an exotic KN resonance $I=1$, $Y=2$ (for which there may be some experimental indication) appears in our model with a width similar to that of $\Delta(1690)$.

Figure 3 shows that the Gell-Mann–Okubo mass formula is also approximately valid for the members of the **27**. Note, however, that the Λ^* resonance appears at a somewhat lower energy. [This is probably due to singlet, **27** mixing (see below).] It can also be seen from Table II and Figs. 3–11 that even though the lower decuplet is very weakly dependent on the F/D ratio, the width and resonance energy of the members of the **27** supermultiplet are much more strongly dependent on it.

In Fig. 5 we give the inverse $g^2/4\pi$ dependence of the resonance energies of the members of the **27** (as well as the other supermultiplets). Note that these resonance energies increase much more rapidly with decreasing coupling constant than the members of the usual decuplet (except for the Λ^*). A linear inverse $g^2/4\pi$ behavior appears only for $g^2/4\pi>100$, and in this region the slope is the same as that of the decuplet.

It is also worthwhile to note that for $g^2/4\pi=14.6$ the **27** appears at an energy of about 5000 MeV, while the lower decuplet then appears at an energy of about 1800 MeV. From our point of view a sensible model must first fit the lower decuplet energies at about the correct experimental values. Thus we use the value $g^2/4\pi=38$ in our calculations, since only then $N_{3/2}^*(1236)$ appears at the correct experimental energy. Since we do not have an arbitrary cutoff parameter in our calculations, we use the coupling constant as the only variable parameter to fit the experimental energies of the members of the lower decuplet. Therefore, we believe that in our model the results corresponding to $g^2/4\pi=38$ are the physical ones.

The only state which does not fit very well into a mass formula of the Gell-Mann–Okubo type is the $\frac{3}{2}^+$ Λ^* state $I=0$, $Y=0$, which could also appear as a singlet. Figure 11 shows that (only in this case) the variation of the F/D ratio changes the phase shifts qualitatively. For the physical value $f=0.33$ there is only one Λ^* resonance in the $\pi\Sigma$ channel at an energy of about 1600 MeV. This appears at lower energies for $f=0.25$, and then there is a second resonance in the $\eta\Lambda$ channel. This one fits better to the other **27** states. Finally, for $f=0.5$, the Λ^* appears again only as a single resonance, but is, however, in the $\bar{K}N$ channel. The critical dependence on the F/D ratio of the Λ^* in case of the baryon exchange contribution is due to the strong f dependence of the potential.[28] The Λ^* state has probably to be interpreted in our model as a singlet-**27** mixing, which is predominantly in the singlet state for an F/D ratio $f=0.33$.

3. Higher $\frac{3}{2}^+$ Resonances

Even though one should not expect the predictions of this simple model to be valid also at very high energies, it is nevertheless amusing to see what happens at such energies. This we do in this section.

At much higher energies than the two lower supermultiplets (namely, at about 3500 MeV) a second decuplet of resonances[29] appears with much broader widths (of about 2000 MeV). In particular, Fig. 6 shows that the Δ state resonates in the πN channel at an energy of about 3182 MeV. Even if we omit the $K\Sigma$ channel, a very broad resonance still occurs in the πN channel at an energy of about 3540 MeV [dotted line in Fig. 6(a)]. Figure 8 shows that in the case of the Σ^* state the $\bar{K}N$ channel resonates at an energy of about 3532 MeV, whereas in the $K\Xi$ channel the eigenphase also goes through 90° at exactly the same energy, but in the wrong direction. This "antiresonance" is a member of a $\bar{1}\bar{0}$ representation of such objects with the additional states $I=0$, $Y=+2$ at an energy of 3070

[28] P. A. Carruthers, *Introduction to Unitary Symmetry* (Wiley-Interscience, Inc., New York, 1966).

[29] Note the difference with the result of strong-coupling theory, which predicts a **35** supermultiplet at about the same energy as the second decuplet appears in our model.

MeV, $N(3660)$, and $I=\frac{3}{2}$, $Y=-1$ at an energy of about 3610 MeV.[30]

For a coupling constant $g^2/4\pi=38$ which fits the $\Delta(1236)$, there are no additional higher $\frac{3}{2}^+$ resonances. It might be worthwhile to mention that for $g^2/4\pi=14.6$ the **27** appears at a very high energy (at about 5000 MeV) and that there is no longer a higher **10** (Fig. 3). On the other hand, Fig. 13 shows that for $g^2/4\pi=100$ a second **27** supermultiplet appears close to the second **10**. It is remarkable that the Gell-Mann–Okubo mass formula also holds approximately for higher supermultiplets. Note that the spacing between consecutive members seems to increase as the average energy of the supermultiplet increases.

In the range $38\leq g^2/4\pi\leq 60$ (where a fit of the fundamental decuplet makes sense), the first three supermultiplets of dimensions **10**, (**1**+**27**), and **10** are present unambiguously and there appear no further resonances at higher energies.

V. COMPARISON WITH EXPERIMENT

The masses, widths, and branching ratios of the usual decuplet were already compared with experiment and with other models in Ref. 8. At present there is not much experimental information on the higher $\frac{3}{2}^+$ resonances. Most phase-shift analyses[31] seem to indicate the presence of a P_{33} ($I=\frac{3}{2}$, $Y=1$) resonance which appears at an energy of about 1690 MeV with a width of about 280 MeV, and is mainly a $K\Sigma$ resonance. In the quark model, this resonance is attributed to a radial quantum number excitation of $\Delta(1236)$ and thus should belong to a decuplet. On the other hand, our model predicts a $K\Sigma$ resonance with the supposed properties to be a member of a **27** $SU(3)$ representation and not of a **10**. Phase-shift analyses seem also to indicate the existence of an N resonance $P_{13}(1860)$ with a width of about 300 MeV. This resonance could be fitted into the $I=\frac{1}{2}$, $Y=+1$ state of our **27**.[32] In addition there are some resonances in the Particle Properties Tables[33] (of still unknown spin) in the energy region in which they would be expected to appear in order to fit into the **27**. These are $\Sigma^*(1690)$ or $\Sigma^*(1780)$ and $\Xi^*(1705)$. However, there seems to be no indication for a Λ^* resonance of sufficiently low energy.[34] Assuming these resonances have all spin $\frac{3}{2}^+$, they could of course fit together with the P_{33} and P_{13} resonances of the pion-nucleon system to an **8** and a **10**.

However, these representations would at present be incomplete and have a missing Λ^*, Ξ, and Ω^-. If we believe in the conclusions of our model, we could predict the above resonances to be members of a **27** and then only the Λ^* would be experimentally missing. (The exotic states will be discussed later.) It is worthwhile to note that in the quark model, whenever there is a Δ resonance one tries to complete it to a decuplet, and whenever there is an N resonance one tries to complete it to an octet. Thus, whenever there is a Δ and an N resonance one needs two Σ^*'s and two Ξ^*'s. However, if both the Δ and N resonances are members of a **27** (as it is the case in our model), one needs only one Σ^* and one Ξ^* to complete the $SU(3)$ supermultiplet. As recently pointed out by Harari,[35] there seems to be experimental indication to the fact that most of the Ξ^*'s and many Σ^*'s which the quark model predicts have as of yet not been found in experiment. This seems to be in support of our model. Of course, our model could probably be ruled out if one finds a second Ω^- at sufficiently low energies, since then $\Delta(1690)$ and Ω^- could be taken as members of the same $SU(3)$ decuplet. On the other hand, if exotic resonances are in fact experimentally found, then one cannot, in general, expect quark-model results to hold also for higher resonances.

Whether exotic resonances exist or not is still an open question. However there are some doubtful candidates for exotic resonances in the Kp channel in the Particle Properties Tables.[33] The $I=1$, $Y=+2$ states $Z_1(1690)$ or $Z_1(1900)$ (which is usually attributed to spin $\frac{3}{2}^+$) could for example belong to a **27** as in our model $Z_1(1609)$ (and have spin $\frac{3}{2}^+$). Other exotic states appear in our model with such large widths that they probably cannot be experimentally observed. The question of the existence of exotic resonances has been frequently discussed in the literature in connection with the concept of duality.[36] Note that in our model, an $I=1$, $Y=+2$ KN resonance of spin $\frac{3}{2}^+$ automatically appears once one performs the dynamical calculation.

So far we have mainly restricted our attention to the resonance behavior of the phase shifts. Next we would like to compare the P_{33} phase shifts obtained in our model with the experimental ones. This is done in Fig. 12, where we also give the results of Ref. 37 in which a Bethe-Salpeter equation for πN scattering was solved by use of Padé approximants. The P_{33} phase shift of our

[30] Further "antiresonances" appear in our model as complete $SU(3)$ multiplets, i.e., two octets at energies between 2000 and 3000 MeV and a decuplet at about 4500 MeV which is connected with the real second decuplet. For perfect input symmetry the two octets of antiresonances appear at the same energy and the real second decuplet and the 10 antiresonances do also.

[31] A. Donnachie, R. G. Kirsopp, and L. Lovelace, CERN Report No. YH838 (unpublished).

[32] Note that Table II shows that both the Δ and N resonances can be made to appear at the correct experimental energies with the correct widths if one chooses the F/D value to be about 0.4.

[33] Particle Data Group, Rev. Mod. Phys. **41**, 109 (1969); A. H. Rosenfeld, UCRL Report No. 18266, 1968 (unpublished).

[34] Note that a similar difficulty arises in the quark model in which a Λ^* is needed in order to complete the octet, and that a low-lying Λ^* is also predicted in $SU(3)''$.

[35] H. Harari, *Proceedings of the Fourteenth International Conference on High-Energy Physics, Vienna, 1968* (CERN, Geneva, 1968), p. 195.

[36] C. Schmid, Phys. Rev. Letters **20**, 969 (1968); R. Dolen, D. Horn, and C. Schmid, Phys. Rev. **166**, 1779 (1968); C. Schmid, CERN Report No. 968, 1969 (unpublished); S. Pinsky, Phys. Rev. Letters **22**, 677 (1969); J. L. Rosner, *ibid.* **21**, 1950 (1968); H. Lipkin, Weizmann Institut report, 1969 (unpublished); R. P. Roy and M. Suzuki, CERN Report No. TH976, 1969 (unpublished).

[37] J. A. Magnaco, M. Pusterla, and E. Remiddi, Saclay Report, 1969 (unpublished).

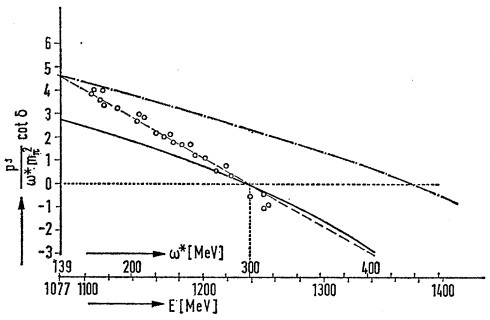

FIG. 14. Chew-Low plot. Plot of $(p^3/\omega m_\pi^2)\cot\delta$ versus $\omega^*=\omega+p^2/2m$ as obtained from our model with $g^2/4\pi=38$ (solid line) and $g^2/4\pi=25$ (dot-dashed line), and as obtained by use of the Chew-Low formula:

$$(p^3/\omega m_\pi^2)\cot\delta=(1/4f^2/3)(1-\omega/\omega_R) \quad \text{with} \quad f^2=0.087$$

(dashed line), which corresponds to the experimental results given by Barnes *et al.*, Phys. Rev. **117**, 225 (1960).

calculation agrees fairly well with experiment near threshold and in the neighborhood of the first resonance, except, of course, at the right-hand side of the resonance position in which the phase shift goes up somewhat slower.[38] In Fig. 14 we compare the experimental Chew-Low plot with that of our model for $g^2/4\pi=38$. Note that the slopes at the resonance position are identical for both, and there is some deviation near threshold. In Fig. 14 we also give the Chew-Low plot calculated from our model for $g^2/4\pi=25$. With this coupling constant we fit the scattering length at threshold. However, the N^* resonance then appears at about 1370 MeV. Note that in the field-theoretic calculation without cutoff of the $\frac{3}{2}^+$ partial wave given in Ref. 39, similar results were obtained.

VI. COMPARISON WITH OTHER THEORIES AND DISCUSSION

Besides the quark model[1,2] and strong coupling[26] (which have already been discussed), there is another model which predicts multiple $SU(3)$ representations in case of spin $\frac{3}{2}^+$. In that model[4] there is besides the usual $SU(3)$ symmetry a further $SU(3)$ degree of freedom, called $SU(3)''$. Except for the usual decuplet, which is assumed to be the lowest supermultiplet, that model predicts for $\frac{3}{2}^+$ a low lying singlet, another decuplet, which is connected with a $\overline{\mathbf{10}}$ supermultiplet (in the manner as described in Fig. 12), a **27**, and in addition two octets (which are degenerate for perfect symmetry). It is remarkable that our model predicts all these supermultiplets for $g^2/4\pi=38$ (see Fig. 3). However, in our calculation the two octets and the $\overline{\mathbf{10}}$ appear as unphysical "antiresonances" (phase shift going down when passing 90°).

In N/D calculations[10,11] second resonances were not predicted. As far as the usual $\frac{3}{2}^+$ decuplet is concerned, the N/D results for the baryon decuplet are similar to the predictions of our model. However, in those calculations the F/D ratio has been usually chosen so as to ensure that the decuplet representation is the only one that is resonant in the low-energy region. Thus, in Ref. 11, F/D was chosen to be 0.35. As discussed in Ref. 10 for values $-2.84<F/D<0.34$, one would also obtain a unitary singlet in addition to the decuplet resonances. In addition (Ref. 10), it is also probable that one would obtain a resonating **27** $SU(3)$ representation in an N/D calculation by choosing $F/D>0.56$.

Even though the baryon exchange diagram is one of the main contributions to the $P_{3/2}$ partial-wave amplitude, it is of course not the only one. Thus if one takes the baryon exchange process as the only contribution to the driving force, as was done in Refs. 8, 10, 11, and in this paper, one has three possibilities to perform the calculation. The first is to do it without a cutoff and with a physical coupling constant $g^2/4\pi=14.6$. One then obtains the resonances at too-high energies and a not-well-satisfied equal-spacing rule for the decuplet. The second possibility is to introduce a cutoff, in which case one fixes the coupling constant at the physical value and adjusts the cutoff to fix $\Delta(1236)$ at the correct experimental energy. However, this has the disadvantage that sometimes one obtains incomplete supermultiplets for some values of the parameters. The third possibility, which was chosen by the authors of Ref. 11 as well as in this paper, is to perform the calculation without a cutoff and to choose the coupling constant as an adjustable parameter chosen so as to fit $\Delta(1236)$ at the correct experimental energy.

Bethe-Salpeter calculations of the baryon spectrum would certainly be of interest.[37] However, the inclusion of spin and $SU(3)$ effects certainly places this problem far beyond the capabilities of present computers.

In summary, the relativistic Schrödinger equation was applied to multichannel pseudoscalar meson-baryon scattering in the $\frac{3}{2}^+$ partial-wave amplitude. The input potential was obtained by computing the baryon exchange contribution to the driving force. Since the Schrödinger equation is an off-shell equation and the potential obtained from a Feynman diagram is known only on-shell, the question arose as to how to perform the extrapolation off the mass shell. We chose to do it in such a way that both initial and final particles are treated symmetrically. In addition, we have made the replacement $a_0+b_0+c_0+d_0\rightarrow 2\sqrt{s}$ (since, as we have already discussed, only the on-shell potential is *a priori* known). In this way we have avoided an arbitrary cutoff parameter in our calculation. Instead we used the coupling constant as an adjustable parameter which we chose to be $g^2/4\pi=38$ in order to obtain $\Delta(1236)$ at the correct experimental energy. The P_{33} phase shifts have been explicitly compared with experiment in Fig. 12.

[38] This is a common disease of all dynamical calculations in which only the baryon exchange force is taken into account and also of many others in which more exchanges are also considered.

[39] L. B. Redei, Nucl. Phys. **1310**, 419 (1969).

Note that they are in qualitative agreement with experiment near threshold and in the neighborhood of the first resonance, except, of course, at the right-hand side of the resonance position, where the phase shift goes up somewhat slower. In Fig. 14 we compared the experimental Chew-Low plot with that of our model. Note that since we started with a large coupling constant, the scattering length predicted by the model differed from experiment by about 30%. However, we still obtained the correct slope at the resonance position and, for example, the calculated P_{33} phase shifts were in qualitative agreement with experiment near threshold and in the neighborhood of the first resonance. Thus, we expect that the phase shifts predicted by the model for somewhat higher energies are also in qualitative agreement with experiment. The model accounted for the usual $\frac{3}{2}^+$ decuplet and predicted the existence of a 27-dimensional $SU(3)$ supermultiplet [to which the experimental $\frac{3}{2}^+$ resonances $\Delta(1690)$, $N(1860)$, $\Sigma(1690)$, or $\Sigma(1780)$, $\Xi(1705)$, and $Z_1(1690)$ or $Z_1(1900)$ might belong, if they were to be confirmed to exist and to have spin $\frac{3}{2}^+$]. In addition, a second $\frac{3}{2}^+$ decuplet was present at much higher energies and with very broad widths. The dependence of the spectrum on the coupling constant was investigated. We found that the lower $\frac{3}{2}^+$ decuplet had an approximately $1/g^2$ dependence in the physical region, while the resonance energies belonging to the **27** and to the higher **10** supermultiplets increased rapidly with decreasing coupling constant.

The dependence of the spectrum on the F/D ratio as well as on $SU(3)$ symmetry breaking was also investigated. It was noticed that the usual decuplet had a very weak F/D dependence, while this was not the case for the resonances belonging to the **27**. For an F/D ratio $f=0.5$ these resonances were about 100 MeV lower than for $f=0.33$, with widths of about a factor of 2 smaller. A value of about $f=0.4$ best fitted the experimental energies and widths of the members of the **27**. In addition, for this value of the F/D ratio the equal-spacing rule for the decuplet was then better fulfilled, and the energy difference between the two Δ resonances became closer to the experimental value. The Gell-Mann–Okubo mass formula for all the $\frac{3}{2}^+$ supermultiplets was in general approximately satisfied when the physical masses for the incoming, outgoing, and exchanged particles were taken, and there was an increase of the mass difference between the different hypercharge members of a given $SU(3)$ representation as the average resonance energy of the supermultiplet increased. In the limit of perfect $SU(3)$ symmetry, the resonances of a given supermultiplet tended to appear at about the same energy.

ACKNOWLEDGMENTS

The authors wish to thank R. Haag for the hospitality at the II Institut in Hamburg. A critical reading of the manuscript by S. Gasiorowicz, F. Gutbrod, and H. Joos is gratefully acknowledged.

In addition, they wish to thank K. Symanzik for pointing out Ref. 39, and the DESY Rechenzentrum for making their IBM 360-75 computing facility available to them.